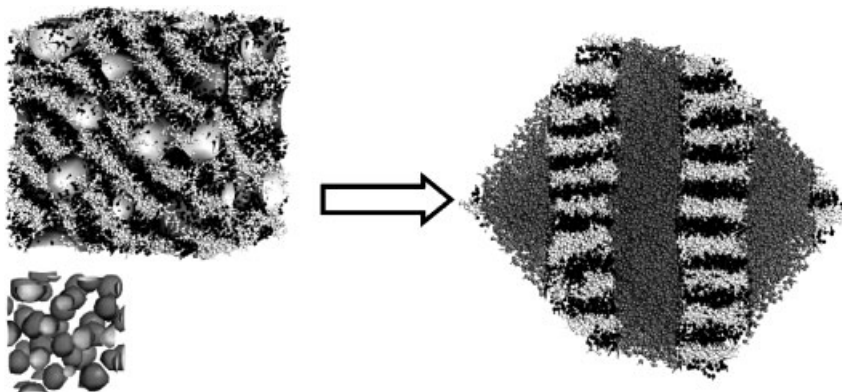# Hierarchical Structure-within-Structure Morphologies in A-*block*-(B-*graft*-C) Molecules

Ching-I Huang,* Yu-Chih Lin

We have used dissipative particle dynamics (DPD) to simulate the self-assembling behavior of A-*block*-(B-*graft*-C) coil-comb molecules, in which each B segment is covalently bonded with one C segment. In addition to the composition, we found that by varying any of the interaction parameters between each pair of components I and J, where $I, J = $ A, B, C, we can also induce a series of morphology transitions associated with two length scales. Moreover, we observed that if the length of the BC-comb block is not long enough, the resulting morphology is mainly in the large-length-scale, ordering between the A-rich and C-rich domains with most of the B in the interfaces. By increasing the length of the BC-comb block, one may expect that both B and C can pack orderly to form a lamellar structure. As a result, various experimentally observed structure-within-structures have been simulated via DPD.

Introduction

Recently, copolymers with hierarchical structure-within-structure morphologies have become a vital and interesting topic, due to their potential applications such as in electrical, optical, and other functional materials.[1,2] Most of the current research has mainly focused on A-*block*-(B-*graft*-C) coil-comb copolymers, in which the component C is typically a short chain molecule and grafted to the backbone B through noncovalent-bonding interactions.[1–11] For instance, Ruokolainen et al.[3–6,11] synthesized a series of polystyrene-*block*-poly(4-vinylpyridine) (PS-*block*-P4VP) copolymers with pentadecylphenol (PDP) as side chains, which they grafted into the P4VP blocks through hydrogen bonds. The resulting coil-comb copolymers, examined by transmission electron microscopy (TEM) and small-angle X-ray scattering (SAXS) displayed a variety of hierarchical structures with two different length scales at room temperature, such as spherical-within- lamellar, cylindrical-within-lamellar, gyroid-within-lamellar, lamellar-within-lamellar, lamellar-within-cylindrical, and lamellar-within-spherical. There, the large-length-scale ordering morphology is mainly driven by segregation between the A-coil blocks and the BC-comb blocks, and hence depends on the block composition. Once the segregation degree between B and C becomes significantly large, a small-length-scale ordering of B and C alternating layers, which typically ranges between 1 and 10 nm, frequently occurs within the original BC-rich domains.

C.-I Huang, Y.-C. Lin
Institute of Polymer Science and Engineering, National Taiwan University, Taipei 106, Taiwan
Fax: +886 2 33665237; E-mail: chingih@ntu.edu.tw

WILEY
InterScience®
DISCOVER SOMETHING GREAT

Indeed, the self-assembling behavior for comb-coil A-*block*-(B-*graft*-C) copolymers, which often exhibit two-length-scale hierarchical structure-within-structure morphologies, may become very complicated as it involves many important parameters, such as the interaction parameters between each pair of components I and J, a_{IJ}, I, $J =$ A, B, C; the compositions of the different components f_A and f_B; the graft density (i.e., the average number of C molecules bonded with one B monomer); and the degree of polymerization N. However, to date, the effects of these parameters on the resulting phase behavior of A-*block*-(B-*graft*-C) copolymers have not yet been addressed theoretically.

We have thus used the newly-developed dissipative particle dynamics (DPD) simulation technique[12,13] to examine the self-assembling behavior of A-*block*-(B-*graft*-C) copolymers. The DPD method has been successfully applied to study the mesophase behavior for a variety of amphiphilic-molecule systems.[12–21] In this work, we have excluded the effects of graft density and assume that each B segment is covalently bonded with one C segment. Our modeled A-*block*-(B-*graft*-C) copolymer chain, as displayed in Figure 1, consists of N_A beads of the A-coil block and $N_B + N_C$ beads of the B-*graft*-C comb block, in which each B and C component has the same number of beads per chain ($N_B = N_C$). The two composition variables, f_A and f_B, are thus reduced down to only one parameter $f_A = N_A/N$, as $f_B = f_C = (1 - f_A)/2$ in our case. Typically, a DPD bead resembles a group of several monomers. Hence, although the total number of beads per chain N in DPD is not the true degree of polymerization, they display a proportional relationship. Among the three interaction parameters, due to the fact that the interaction parameters a_{AB} and a_{BC} play a dominant role in the large length scale and small length scale of segregations, respectively, we let $a_{AC} = a_{BC}$ to reduce one interaction variable. Accordingly, here we aim to illustrate how the resulting morphology formation, in particular the experimentally observed structure-within-structure, is affected by a_{AB}, $a_{AC} = a_{BC}$, f_A, and the total degree of polymerization N.
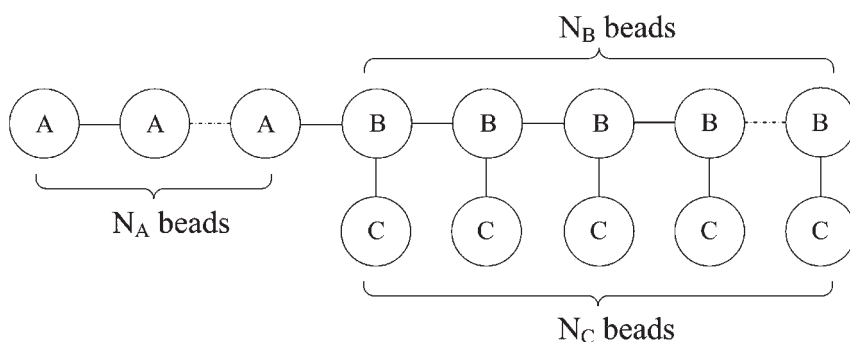
DPD Simulation Method and Model Parameters

The DPD simulation method was originally proposed by Hoogerbrugge and Koelman[12] and first applied successfully by Groot and Madden[14] on the microstructures in linear AB diblock copolymer melts. The detailed formula can be found in ref.[13–14], and will not be reiterated here. We previously have employed DPD to examine the phase separation behavior for amphiphilic molecules in the presence of solvents,[20,21] in which the details of DPD were also given.

In simulating the phase behavior of A-*block*-(B-*graft*-C) copolymers by DPD, the particle mass m, the cut-off radius r_c, and the temperature k_BT were all set equal to 1, for convenience. The parameters γ and σ, which occur in the dissipative force and random force, respectively, were set to 4.5 and 3.0, respectively.[13] The connecting pairs of beads in a molecule were assumed to interact via a linear spring with a harmonic spring constant C equal to 4.[13] We set the particle density ρ equal to 3, and hence the dimensionless interaction parameter (that is, in terms of k_BT) between equal particles $a_{II} = 25$.[13] The interaction parameter between different components I and J can be estimated by the relationship between a_{IJ} and the Flory-Huggins interaction parameter χ_{IJ} derived by Groot and Warren[13] for $\rho = 3$, $a_{IJ}(T) = a_{II} + 3.497\chi_{IJ}(T)$. Therefore, the value of $a_{IJ} \leq 25$ corresponds to $\chi_{IJ} \leq 0$, which indicates that components I and J are very miscible. As the incompatibility between I and J increases, a_{IJ} increases from 25.

The DPD simulations were started with an initially-disordered configuration and performed in a 3-D lattice of size L^3 grids. Note that in order to exclude the finite-size effects on the resulting morphology patterns, we had to perform the DPD simulations in different sizes of the simulation box until the structures were no longer affected. As expected, the longer the copolymer chain, the larger the simulation box size. In the current work, the box size ranges from $15 \times 15 \times 15$ to $30 \times 30 \times 30$ for $N = 10$ to 25 studied here. The DPD simulations were carried out by integrating the positions and velocities of all beads according to the velocity-Verlet algorithm with $\lambda = 0.65$ and the time step equal to 0.05.[22]

Results and Discussion

Effects of the Interaction Parameters a_{AB} and $a_{AC} = a_{BC}$

In order to explore the effects of the interaction parameter a_{AB} on the microstructures formed in A-*block*-


Figure 1. A schematic plot of the model A-*block*-(B-*graft*-C) coil-comb molecules.

(B-*graft*-C) coil-comb molecules, we chose $f_A = 0.2$, $N = 10$, $a_{AC} = a_{BC} = 70$, and varied the value of a_{AB} from 0 to 120. Figure 2 displays the resulting morphology transition from segregated AB and C lamellae, $L_{AB,C}$, $(0 \leq a_{AB} \leq 25) \rightarrow$ gyroid of A, G_A, $(a_{AB} = 30) \rightarrow$ hexagonally-packed A-formed cylinders, C_A^{HEX}, $(35 \leq a_{AB} \leq 70) \rightarrow$ A-formed spheres, S_A,

$(a_{AB} = 75) \rightarrow$ A-formed spheres within the segregated B and C lamellae, S_A-within-$L_{B,C}$, $(80 \leq a_{AB} \leq 120)$. The interaction parameters a_{AC} and a_{BC} were chosen to be 70 initially, which is large enough for both the A and B components to tend to segregate with C. Accordingly, when $a_{AB} \leq 25$, that is when A and B are highly miscible, the microstructure formed by the system is mainly caused by segregation between AB and C, and therefore, a stable $L_{AB,C}$ is observed for the system with comparable values of volume fractions of AB and C. As a_{AB} increases, due to the fact that the immiscibility degree between A and B becomes more significant, the B component gradually departs from the original AB-rich domains into the interfaces between A-rich and C-rich domains. This behavior is analogous to decreasing the effective composition in the AB-rich domains, and thus a transition from $L_{AB,C} \rightarrow G_A \rightarrow C_A^{HEX} \rightarrow S_A$ occurs with an increase in a_{AB}. Furthermore, it is interesting to observe that when a_{AB} keeps increasing so that most of the B chains are pushed towards the C-rich domains, the significant degree of incompatibility between B and C enables a small-length-scale B and C segregated lamellar phase to be formed within the large-length-scale BC-rich matrix.

A series of morphology transitions associated with two length scales can be induced by not only varying the interaction parameter a_{AB} but also varying the value of $a_{AC} = a_{BC}$. To illustrate this, we first performed the DPD simulations by varying $a_{AC} = a_{BC}$ for $f_A = 0.2$, $N = 10$, and with a_{AB} fixed at a larger repulsion value of 100. As can be seen clearly in Figure 3(a), a series of transitions from $S_A \rightarrow S_A$-within-$L_{B,C} \rightarrow C_A$-within-$L_{B,C}$ occurs with an increase in $a_{AC} = a_{BC}$ from 50 to 70 to 80, respectively. It is not surprising that the small-length-scale B and C lamellae are formed on increasing the interaction parameter between B and C. Moreover, simultaneously increasing the value of a_{AC} and a_{BC} may also enhance the segregation of B from C towards A, and thus cause a large-length-scale morphology transition towards increasing the effective
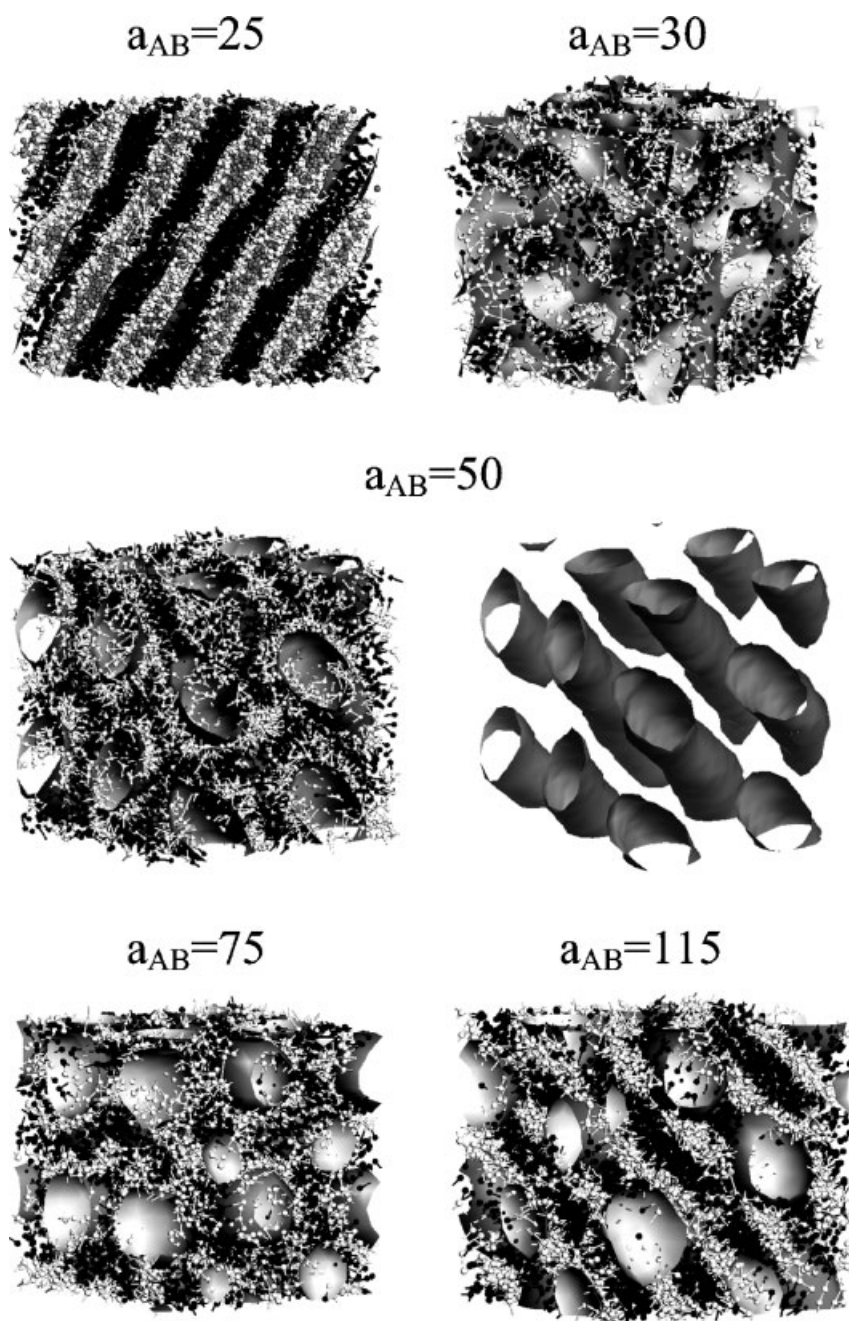
Figure 2. Morphology variation of A-*block*-(B-*graft*-C) molecules with a_{AB} when $N = 10$, $f_A = 0.2$ and $a_{AC} = a_{BC} = 70$, simulated in a box of size $15 \times 15 \times 15$. The white and black colors represent B and C, respectively. For clarity, we omit the A beads and use the gray surface to represent the isosurface of component A.
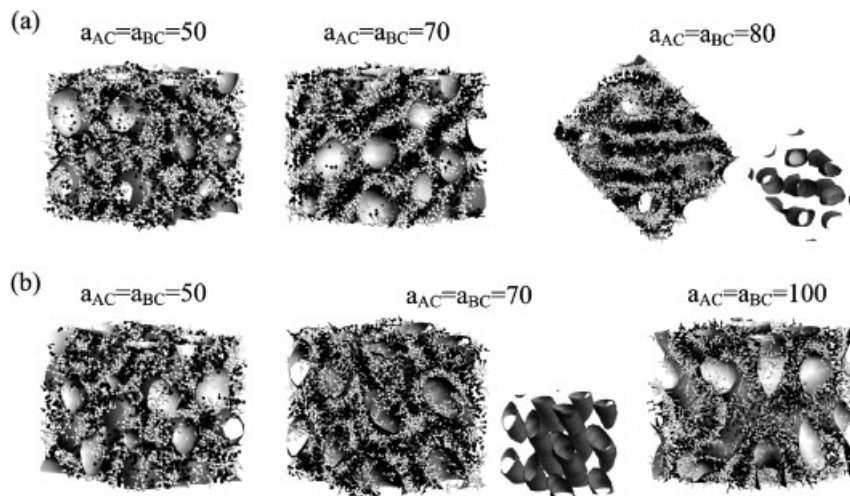
Figure 3. Morphology variation of the A-*block*-(B-*graft*-C) molecules with $a_{AC} = a_{BC}$ when $N = 10$, $f_A = 0.2$ and a_{AB} equal to (a) 100 and (b) 50, respectively, simulated in a box of size $15 \times 15 \times 15$. The white and black colors represent B and C, respectively. For clarity, we omit the A beads and use the gray surface to represent the isosurface of component A.

composition of A from S_A to C_A^{HEX}. A similar trend of morphology transitions at large length scales from $S_A \rightarrow C_A^{HEX} \rightarrow G_A$ on increasing $a_{AC} = a_{BC}$ from 50 to 70 to 100, respectively, has also been observed for the same system, with a_{AB} set at a smaller value of 50, as displayed in Figure 3(b). However, in this case we observed no evidence of the existence of the structure-within-structure, even increasing $a_{AC} = a_{BC}$ up to a high value of 100. These results point to the fact that, in order to form the small-length-scale lamellar segregation between B and C within the large-scale BC-rich domains, the interaction parameters between B and C (a_{BC}) and also the interaction parameters between the A-coil block and the BC-comb block (a_{AB} and a_{AC}) both have to be significantly large. Otherwise, the continuous increase in $a_{AC} = a_{BC}$ only causes B to move towards the interfaces between the A-rich domains and C-rich domains, and trigger a morphology transition at the large length scale that we observe in Figure 3(b).

**Effects of Composition f_A and Chain Length N**

Finally, we wanted to investigate whether the DPD simulations can show the various types of structure-within-structures by varying the composition f_A, as have been frequently observed in experiments.[4] To illustrate this, we chose $a_{AC} = a_{BC} = 70$ and $a_{AB} = 100$. Figure 4 displays the resulting DPD-simulation results at $f_A = 0.1$, 0.3, 0.4, 0.5, and 0.6, and $N = 10$–25. Generally speaking, on increasing the A composition, f_A, the large-length-scale morphology formed changes from $S_A \rightarrow C_A^{HEX} \rightarrow G_A \rightarrow L$, as

expected. More interestingly, we observed that the formation of small-length-scale segregation between B and C within the BC-rich domains is dependent on the chain length N and f_A (more precisely, on the length of the BC-comb block). When $f_A = 0.1$, the system forms the S_A-within-$L_{B,C}$ morphology, regardless of whether the value of N is 10 or 20, and yet increasing N makes the separation between B and C more evident. However, when $f_A > 0.1$, we found that the systems with $N = 10$ are not be able to form any structure-within-structure, but only align to form A-rich and C-rich segregated domains with B in the interfaces. Indeed, this is reasonable due to the fact that when the length of the BC-comb block becomes short, the segregation degree between B and C is not significant enough to make the B and C blocks well-aligned to form lamellae. Thus, the resulting morphology is mainly driven by the segregation between A and C, and B acts more like a component in the interfaces. By increasing the length of the BC-comb block, one may expect that B and C will separate evidently, and form a lamellar structure. For example, when N increases to 20, both types of hierarchical structures of C_A^{HEX}-within-$L_{B,C}$ ($f_A = 0.3$, 0.4) and $L_{B,C}$-within-$L_{A,BC}$ ($f_A = 0.5$), are observed. When f_A increases to 0.6, though the small-length-scale B and C lamellae are not well formed within the BC-rich lamellae for $N = 20$, the formation of $L_{B,C}$-within-$L_{A,BC}$ is still clearly observed as N increases to 25. These simulated structure-within-structures, in which the small-length-scale lamellae are typically perpendicular to the large-length-scale structures, are in good agreement with those observed experimentally in A-*block*-(B-*graft*-C) coil-comb copolymers. Note that we have not obtained other types of structure-within-structures, such as $L_{B,C}$-within-C_{BC} and $L_{B,C}$-within-S_{BC}. This is mainly due to the fact that these hierarchical structures are formed when f_A is larger (i.e., the comb composition is smaller). Accordingly, the total chain length N has to increase further in order to generate the small-length-scale lamellar ordering.

Conclusion

We have successfully applied DPD simulations to show that the formation of the hierarchical structure-within-structures in A-*block*-(B-*graft*-C) coil-comb molecules is strongly influenced by the A composition f_A, the
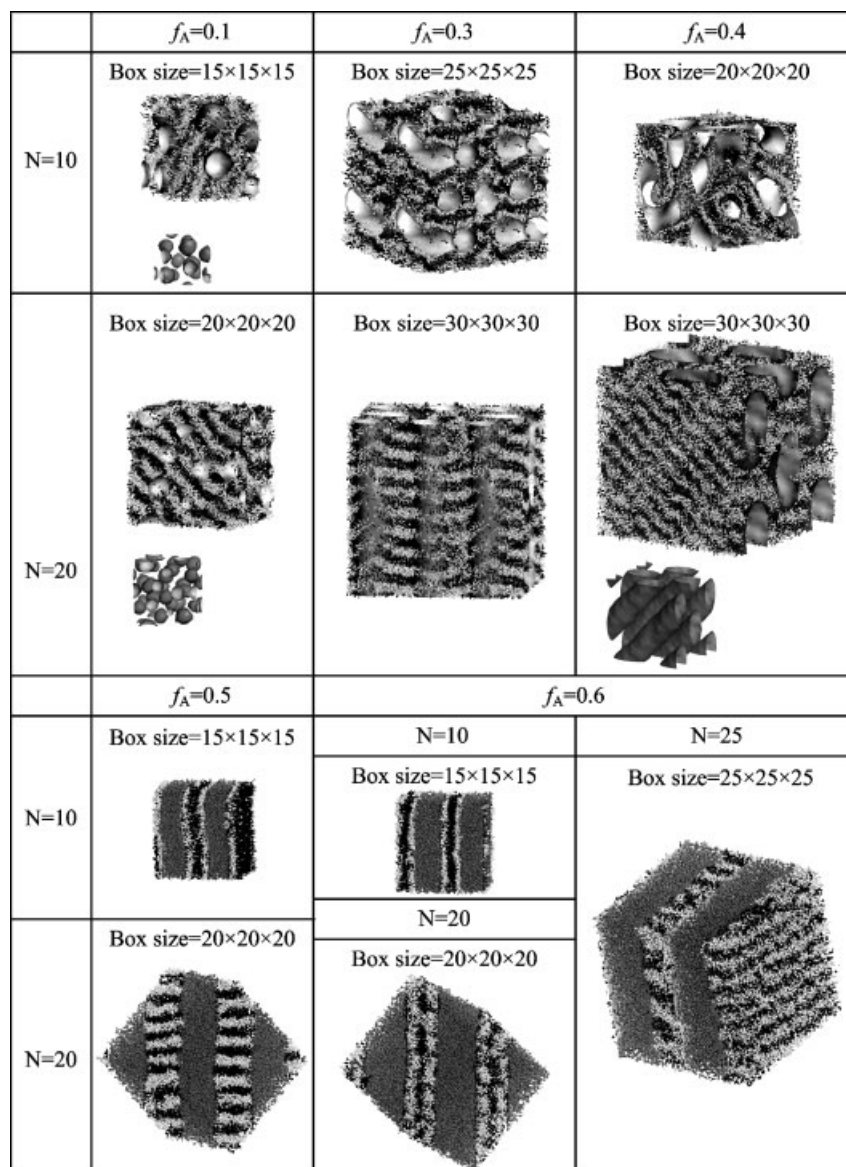
Figure 4. Morphology variations of A-*block*-(B-*graft*-C) molecules with f_A and N at $a_{AC} = a_{BC} = 70$ and $a_{AB} = 100$. The white and black colors represent B and C, respectively. For clarity, we omit the A beads and use the gray surface to represent the isosurface of component A.

total chain length N, and the interaction parameters between each pair of components I and J, where $I, J =$ A, B, C. As expected, f_A has a great influence on the geometry of large-length-scale microstructures. Varying any of the interaction parameters can also induce a series of morphology transitions at the large length scale. In order to form the small-length-scale segregated lamellae within the large-length-scale structures, not only the immiscibility degrees between B and C but also those between the A-coil block and the BC-comb block are significant. In addition, we observe that the chain length N has a great influence on the formation of hierarchical structure-within-structures. When N is small, since the length of the BC-comb block is not long enough to ensure the

formation of well-ordered B and C lamellar segregation, the resulting morphology is mainly in the large-length-scale ordering, with most of the B segregated along the interfaces between the A-rich and C-rich domains. With an increase in the chain length N, various experimentally observed structure-within-structures, such as S_A-within-$L_{B,C}$, C_A^{HEX}-within-$L_{B,C}$, and $L_{B,C}$-within-$L_{A,BC}$, have been simulated via DPD by increasing the composition f_A.

[1] O. Ikkala, G. ten Brinke, *Chem. Commun.* **2004**, 2131.
[2] G. ten Brinke, O. Ikkala, *Chem. Rec.* **2004**, *4*, 219.
[3] J. Ruokolainen, R. Makinen, M. Torkkeli, T. Makela, R. Serimaa, G. ten Brinke, O. Ikkala, *Science* **1998**, *280*, 557.
[4] J. Ruokolainen, G. ten Brinke, O. Ikkala, *Adv. Mater.* **1999**, *11*, 777.
[5] J. Ruokolainen, M. Saariaho, O. Ikkala, G. ten Brinke, E. L. Thomas, M. Torkkeli, R. Serimaa, *Macromolecules* **1999**, *32*, 1152.
[6] T. Ruotsalainen, M. Torkkeli, R. Serimaa, T. Makela, R. Maki-Ontto, J. Ruokolainen, G. ten Brinke, O. Ikkala, *Macromolecules* **2003**, *36*, 9437.
[7] C. S. Tsao, H. L. Chen, *Macromolecules* **2004**, *37*, 8984.
[8] E. Polushkin, S. Bondzic, J. de Wit, G. A. van Ekenstein, I. Dolbnya, W. Bras, O. Ikkala, G. ten Brinke, *Macromolecules* **2005**, *38*, 1804.
[9] A. Laiho, R. H. A. Ras, S. Valkama, J. Ruokolainen, R. Osterbacka, O. Ikkala, *Macromolecules* **2006**, *39*, 7648.
[10] W. van Zoelen, G. Alberda van Ekenstein, O. Ikkala, G. ten Brinke, *Macromolecules* **2006**, *39*, 6574.
[11] S. Valkama, T. Ruotsalainen, A. Nykanen, A. Laiho, H. Kosonen, G. ten Brinke, O. Ikkala, J. Ruokolainen, *Macromolecules* **2006**, *39*, 9327.
[12] P. J. Hoogerbrugge, J. M. V. A. Koelman, *Europhys. Lett.* **1992**, *19*, 155.
[13] R. D. Groot, P. B. Warren, *J. Chem. Phys.* **1997**, *107*, 4423.
[14] R. D. Groot, T. J. Madden, *J. Chem. Phys.* **1998**, *108*, 8713.
[15] E. Ryjkina, H. Kuhn, H. Rehage, F. Muller, J. Peggau, *Angew. Chem., Int. Ed.* **2002**, *41*, 983.
[16] S. Yamamoto, Y. Maruyama, S. Hyodo, *J. Chem. Phys.* **2002**, *116*, 5842.
[17] D. Liu, C. Zhong, *Macromol. Rapid Commun.* **2005**, *26*, 1960.
[18] H. J. Qian, Z. Y. Lu, L. J. Chen, Z. S. Li, C. C. Sun, *Macromolecules* **2005**, *38*, 1395.
[19] J. Xia, C. Zhong, *Macromol. Rapid Commun.* **2006**, *27*, 1110.
[20] C. I. Huang, Y. J. Chiou, Y. K. Lan, *Polymer* **2007**, *48*, 877.
[21] C. I. Huang, H. Y. Hsueh, Y. K. Lan, Y. C. Lin, *Macromol. Theory Simul.* **2007**, *16*, 77.
[22] M. P. Allen, D. J. Tildesley, "Computer Simulation of Liquids", Clarendon, Oxford 1987.